8 The linear analysis as applied to a squeeze film bearing is only valid for small displacements. The squeeze film bearing support which is used on a number of gas turbine designs is highly nonlinear in its behavior and will not function under certain ranges of unbalance and unidirectional loading.

Acknowledgments

The author wishes to acknowledge the support and encouragement of Robert L. Cummings and Erwin Zaretsky of NASA Lewis Research Center, Cleveland, on the development of this paper, P. De Choudhury for his assistance on programming, and particularly, R. Gordon Kirk for his efforts on the Rotor 4P, 4M, and the squeeze-film bearing programs. The study was supported in part by NASA Grant NGR 47-005-050 and NASA Institutional Grant NsG-682, University of Virginia.

References

1 Alford, J. S., "Protecting Turbomachinery From Self-Excited Rotor Whirl," *Journal of Engineering for Power*, Trans. ASME, Series A, No. 4, Oct. 1965, pp. 333–344.

2 Kulina, M., "A New Concept for Critical Speed Control," SAE National Aeronautic Meeting, New York, N. Y., April 24–27, 1967.

3 Dworski, J., "High-Speed Rotor Suspension Formed by Fully Floating Hydrodynamic Radial and Thrust Bearings," *Journal of Engineering for Power*, Trans. ASME, Series A, No. 2, Apr. 1964, pp. 149–160.

4 "New Squeeze Bearing Mount," Rocketdyne Corporation, Product Engineering, March 28, 1960.

5 Van Nimwegen, Robert R., "Critical Speed Problems Encountered in the Design of High Speed Turbomachinery," SAE, Oct. 1964, pp. 524–536.

6 Hamburg, G., and J. Parkinson, "Gas Turbine Shaft Dynamics," *SAE Transactions*, Vol. 70, 1962, pp. 774–784.

7 Suter, P., "Bearing Flexibility and Damping at the First Critical Speed," *Sulzer Technical Review 3*, 1962.

8 Linn, F. C., and Prohl, M. A., "The Effect of Flexibility of Support Upon the Critical Speeds of High-Speed Rotors," *Trans. SNAME*, Vol. 59, 1951, pp. 536–553.

9 Cooper, S., "Preliminary Investigation of Oil Films for Control of Vibration," *Proceedings of the Lubrication and Wear Convention*, I. Mech. E. 1963, London, England.

10 *Aviation Week* and *Space Technology*, Feb. 6, 1967, p. 39.

11 Wood, W. J., "Non-Linear Vibration Damping Functions for Fluid Film Bearings," SAE Paper, 1966.

12 Ng, C. W., and Orcutt, F. K., "Steady State and Dynamic Properties of the Floating-Ring Journal Bearing," Journal of Lubrication Technology, Trans. ASME, Series F, Vol. 90, No. 1, Jan. 1968, pp. 243–253.

13 Myklestad, N. O., "A New Method of Calculating Natural Modes of Uncoupled Bending Vibration of Airplane Wings and Other Types of Beams," *Journal of Aeronautical Sciences*, Apr. 1944, pp. 153–162.

14 Gunter, E. J., "Dynamic Stability of Rotor-Bearing Systems," NASA SP-113, Office of Technical Utilization, U. S. Government Printing Office, Washington, D. C., 1966.

DISCUSSION

J. M. McGrew[2]

In recent years, jet engine manufacturers both here and abroad have added various forms of squeeze film bearings in series or parallel with conventional rolling element bearings to minimize the effect of unbalance on system response. The author has presented an analysis of the effect of support damping and stiffness on the dynamic response of such a hypothetical rotor-bearing system.

The author emphasizes in the paper title and in the text that machinery using rolling element bearings is being considered. As a result of considering only rolling element bearings, the author makes a number of legitimate assumptions which simplify his theoretical derivations. However, the analytical model which the author ends up with for the squeeze-film supported rolling element bearing is identically the same as the analytical model which is obtained for a rigidly supported fluid-film bearing.

[2] Mechanical Technology Inc., Latham, N. Y.

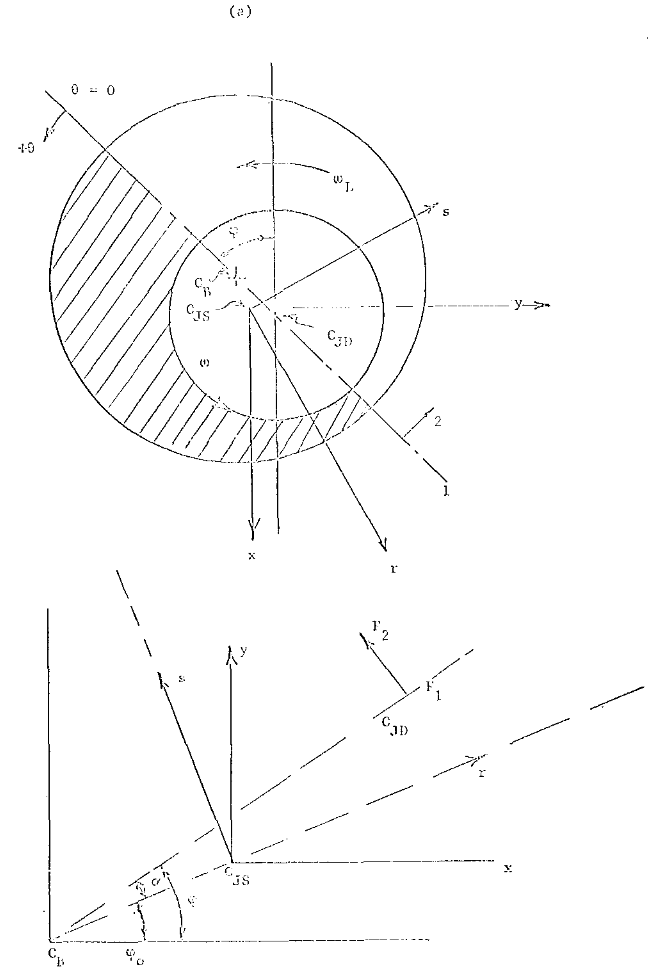

Fig. 15 Nomenclature

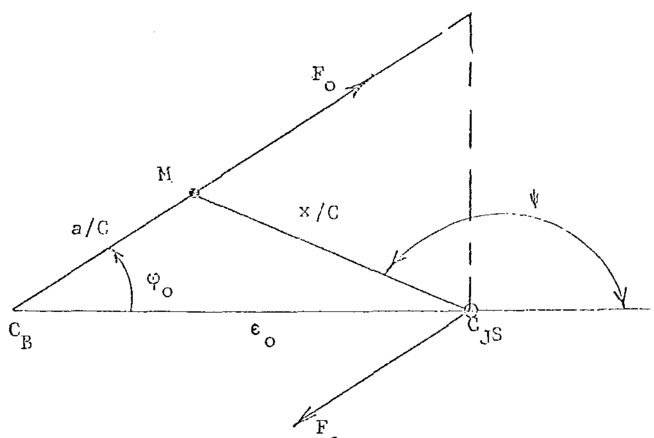

Fig. 16

A number of rotor dynamic analyses have already been published which treat fluid-film two-bearing machines, with either rigid and flexible rotors, where each bearing is represented by 8 (or in general, 16) linearized coefficients. Lund and Sternlicht [15][3] have studied the effect of transmitted forces for a two bearing machine having a symmetric single-mass flexible rotor. Lund

[3] Numbers in brackets designate Additional References at end of Discussion (and Closure).

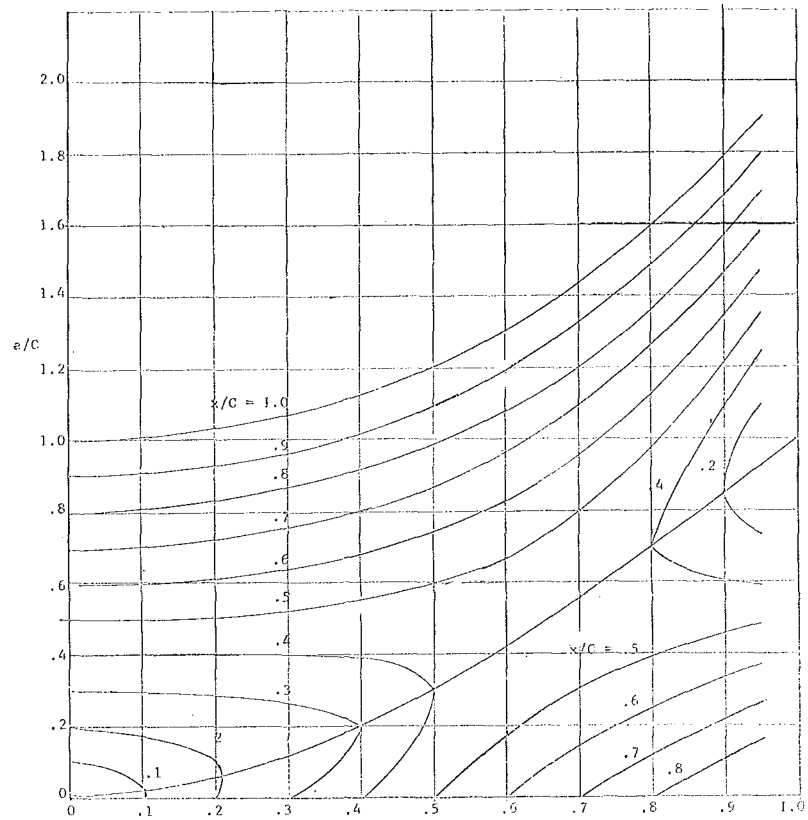

Fig. 17 Possible value of a/C versus eccentricity for various unbalance levels

[16] has also studied the attenuation of transmitted bearing forces for an unbalanced, flexible, symmetrical, two-mass rotor supported in fluid-film bearings which in turn are mounted in flexible, damped supports. Each bearing is characterized by 4 spring and 4 damping coefficients. This analysis is a more general case than the author's present analysis, although it is limited to a symmetrical rotor while the author's analysis can treat a non-symmetrical rotor (provided that it is rigid).

Lund, in [16] and [17], includes the effect of bearing support mass. In [16] he points out that while a soft mount is desirable for reducing transmitted forces, the "support resonance" due to the support mass may become important under soft mount conditions. The author's present analysis does not permit investigation of "support resonance" effects because support mass is neglected. These effects are particularly important in jet engine design where casing resonances are as serious a problem as rotor resonances.

The one significant advantage of the author's work over previous work is that non-symmetric rotors can be handled providing the rotor acts as a rigid body in the speed range of interest.

The author presents his analytical results for a range of damping values. However, no mention is made in the text as to the actual range of damping which may be obtained from a practical squeeze film support bearing.

A simple approach to calculate squeeze film damper performance is to make use of the short bearing approximation. This is valid since most practical dampers have a very low L/D ratio. The author assumes a linear treatment by considering small oscillations about a static equilibrium position (author's equations (8) and (9)). An alternative approach is to adopt a quasi-linear model by considering small oscillations about a quasi-static equilibrium position, a circular orbit. Neither of these may be a legitimate assumption. A true representation of the oil film would require a nonlinear model.

However, for illustration purposes, consider the journal oscillating about a quasi-static equilibrium position C_{JS} in Fig. 15. The instantaneous journal center is C_{JD}. It can be shown that for a "short" journal bearing with 180-deg film extent, the dynamic oil film forces acting on the journal can be expressed as

$$F_r = -C_{rr}\dot{r} - k_{rr}r + C_{rs}\dot{s} - k_{rs}s + F_{1_0} \quad (27)$$

$$F_s = C_{sr}\dot{r} - k_{sr}r - C_{ss}\dot{s} - k_{ss}s + F_{2_0} \quad (28)$$

where

$$\frac{Ck_{rr}}{F_0} = \frac{8(1 + \epsilon_0^2)}{(1 - \epsilon_0^2)[\pi^2(1 - \epsilon_0^2) + 16\epsilon_0^2]^{1/2}} \quad (29)$$

$$\frac{Ck_{rs}}{F_0} = \frac{\pi(1 - \epsilon_0^2)^{1/2}}{\epsilon_0[\pi^2(1 - \epsilon_0^2) + 16\epsilon_0^2]^{1/2}} \quad (30)$$

$$\frac{Ck_{sr}}{F_0} = \frac{\pi(1 + 2\epsilon_0^2)}{\epsilon_0(1 - \epsilon_0^2)^{1/2}[\pi^2(1 - \epsilon_0^2) + 16\epsilon_0^2]^{1/2}} \quad (31)$$

$$\frac{Ck_{ss}}{F_0} = \frac{4}{[\pi^2(1 - \epsilon_0^2) + 16\epsilon_0^2]^{1/2}} \quad (32)$$

$$C_{rs} = C_{sr} = -\frac{k_{ss}}{\omega_L} \quad (33)$$

$$C_{ss} = -\frac{k_{rs}}{\omega_L} \quad (34)$$

$$C_{rr} = -\frac{k_{sr}}{\omega_L} \quad (35)$$

$$F_{1_0} = \frac{\mu L^3 R}{C^2}\left[\frac{(\bar{\omega} - 2\omega_L)\epsilon^2}{(1 - \epsilon^2)^2}\right] \quad (36)$$

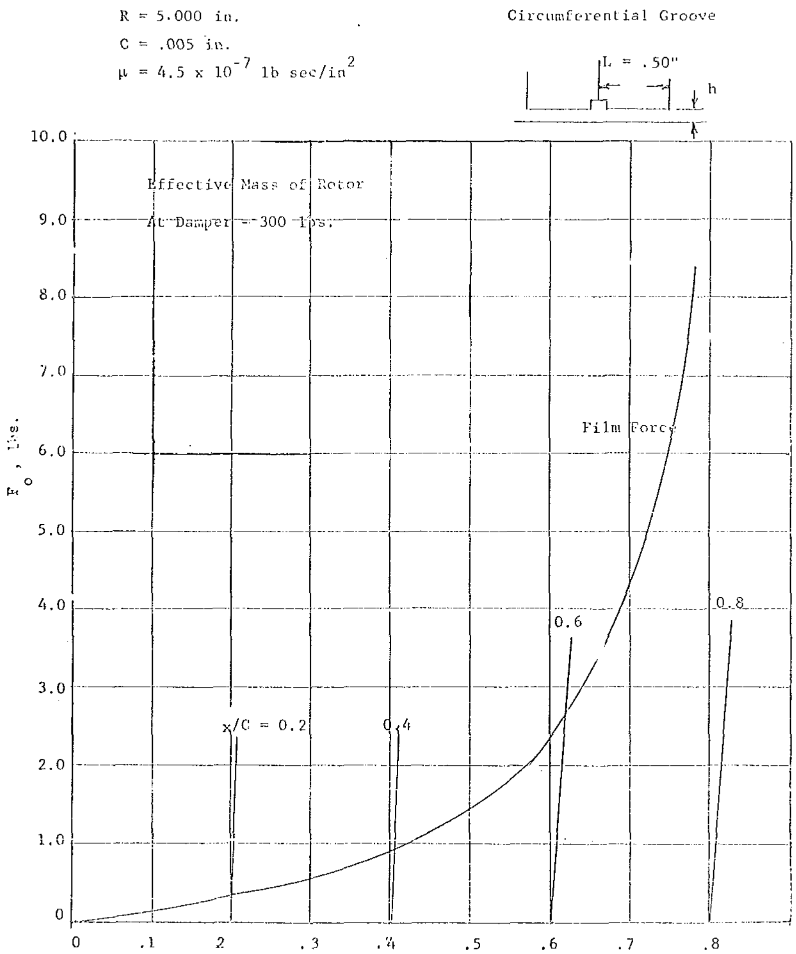

Fig. 18 Sample quasi-steady state equilibrium calculation

$$F_{2_0} = \frac{\mu L^3 R}{4C^2}\left[\frac{(\bar{\omega} - 2\omega_L)\pi\epsilon}{(1 - \epsilon^2)^{3/2}}\right] \tag{37}$$

and the attitude angle is given by

$$\varphi_0 = \tan^{-1}\left[\pi/4\,\frac{(1 - \epsilon_0^2)^{1/2}}{\epsilon_0}\right] \tag{38}$$

The equation of motion for a mass mounted in a damper is

$$M(\ddot{r} - \omega^2(r + x_1 + e_0) - 2\dot{s}\omega) = F_r \tag{39}$$

$$M(\ddot{s} - (s + x_2)\omega^2 + 2\dot{r}\omega) = F_s$$

The equations of motion plus the film force equation lead to a fourth order frequency equation which is governed by the nondimensional parameters $F_0/MC\omega^2$ and ϵ_0. A relatively simple analysis allows for the solution of the frequency equation and the prediction of the regions of instability. Both the threshold of stability and unbalance response can be calculated using the short bearing approximation.

A simplification results if it is assumed

$$\dot{\epsilon} = \dot{\varphi} = 0$$

which is equivalent to a nonrotating squeeze film damper in which the center orbits in a circle with constant attitude angle. For this case the spring coefficient is given by

$$k_0 = \frac{F_{2_0}}{C\epsilon_0} = \frac{2\mu\omega L^3}{C^3}\,\frac{\epsilon_0}{(1 - \epsilon^2)^2} \tag{40}$$

and the damping term by

$$C_0 = \frac{F_{1_0}}{C\omega\epsilon_0} = \frac{\mu L^3 R}{2C^3}\,\frac{\pi}{(1 - \epsilon_0^2)^{3/2}} \tag{41}$$

Equations of Equilibrium—Quasi-Static Case. The force generated in the fluid film must be equal and opposite to the dynamic unbalance force in order to satisfy equilibrium. The conditions for balance of the quasi-static-state forces on the journal for a given unbalance are shown in Fig. 17.

From the geometry of Fig. 16 the relation between a/C, x/C and ϵ_0

$$a/C = \epsilon_0 \cos\varphi_0 \pm \sqrt{(x/C)^2 - (\epsilon_0 \sin\varphi_0)^2} \tag{42}$$

where φ_0 is given by equation (38). Fig. 17 shows the possible values of $\frac{a}{C}$ as a function of ϵ with $\frac{x}{C}$ as a parameter. It will be noticed that for some values of ϵ, there are two values of $\frac{a}{C}$, an inner and outer mode.

From $\frac{a}{C}$ and an estimate of the effective rotor mass at the damper the inertia force can be calculated from

$$F = Ma\omega^2 \tag{43}$$

At equilibrium the inertia force must balance the film force. Fig. 18 shows a sample set of equilibrium curves showing possible running conditions for a range of unbalance eccentricities and a stated geometry. The intersection of the inertia curve and the film force curve establish a possible operating condition. For a given unbalance x, this process can be repeated for a range of speeds and the amplitude response and phase angle ψ determined as a function of operating speed.

Effect of Oil Supply. The previous discussions have assumed a film extent in the damper of 180 deg. This is a reasonable assumption for moderate supply pressures. If the supply pressure is increased above moderate levels, the film will extend beyond 180 deg and the bearing will approach the Sommerfeld condition, that is the radial component of force F_{20} will approach 90 deg. This has been observed by Cooper [9]. He also noted that this effect is most predominant in damper bearings of low L/D ratio. Both supply pressure (i.e., film extent) and L/D ratio will affect damper performance.

In practice, it is found that the quasi-static model using the short bearing approximation provides a reasonable tool for designing damper bearings. A rule of thumb based on Fig. 17 is that damper clearance should run about 2 to 3 times x (see Fig. 18).

There are basically two theories for explaining squeeze film effectiveness (1) isolation and (2) damping. The isolation school states that squeeze film effectiveness is due primarily to isolation, i.e., by centering the rotor mass c.g. at the bearing axis. The other school argues that damping is the primary influence on squeeze film effectiveness. Would the author comment?

I also would question how the author arrived at the spring and damping coefficients for the sample design case in Figs. 13 and 14. Since damper performance is relatively insensitive to L/D ratio why was an L/D as large as 0.5 used? What was the assumed oil supply pressure and method of feeding as these will significantly effect the film spring and damping properties (i.e., film extent)?

Lastly, the author is to be congratulated on presenting a well written and interesting paper which is a significant contribution to the rotor-dynamics literature.

Additional References

15 Lund, J. W., and Sternlicht, B., "Rotor-Bearing Dynamics With Emphasis on Attenuation," *Journal of Basic Engineering*, Trans. ASME, Series D, Vol. 84, No. 4, 1962, pp. 491–502.

16 Lund, J. W., "Attenuation of Bearing Transmitted Noise—Volume 2, Part 1: Attenuation of Rotor Unbalanced Forces by Flexible Bearing Supports," Report No. EC 232, prepared for Bureau of Ships under Contract NOBs-86914, Aug. 1964.

17 Lund, J. W., "The Stability of an Elastic Rotor in Journal Bearings With Flexible, Damped Supports," *Journal of Applied Mechanics*, Trans. ASME, Vol. 87, Series E, 1965, pp. 911–920.

F. A. Shen[4]

The analysis conducted by Dr. Gunter is a useful one toward the understanding of optimum bearing mounting stiffness and damping requirements in achieving a smooth running rotor over a predetermined speed range. The author is to be commended for his work in providing interesting numerical illustrations of the optimum bearing mounting characteristics for a rotor-bearing system.

The technique of incorporating a substantially lower bearing mounting stiffness with or without damping in eliminating severe bearing reactions and shaft deflections for a speed range has been frequently applied in the design of a rotor-bearing system.

To gain insight into the mechanism of bearing mounting stiffness and damping in affecting the rotor deflection and bearing reactions, an example of a rigid, single-mass rotor symmetrically supported on two identical, force characteristic bearings is used. In such a case, the rotor deflection to mass eccentricity ratio, $\frac{r}{e}$, at its critical speed may be represented by equation (44).

$$\frac{r}{e} = \frac{M\omega_n}{C} \tag{44}$$

where M is the rotor mass; ω_n, the undamped critical speed; and C, the bearing damping coefficient.

The total two bearing reaction, F, at the critical speed can then be written as:

$$F = M\omega_n^2 e \left[\left(\frac{M\omega_n}{C} \right)^2 + 1 \right]^{1/2} \tag{45}$$

Equation (41) clearly indicates that the bearing reaction is a strong function of the magnitude of the critical speed. To minimize the bearing reaction, an effective way would be to reduce the critical speed by using a low bearing stiffness. In-asmuch as it is not always practical to lower the support bearing stiffness because of load capacity or life expectancy limitations of rolling-element bearings, a resilient bearing mount inserted between bearing and housing has been found effective in reducing the system critical speed; and, consequently, the bearing reactions. With the single-mass system, it can be shown that at a speed above $\sqrt{2}\omega_n$ the bearing reactions increase with the damping coefficient similar to that found by the author.

An additional parameter which also affects the smooth running performance of a rotor at or near a critical speed is the rotor spin acceleration encountered during startup or variable speed operation. According to Macchia [18], the maximum rotor deflection at the critical speed for a single-mass, undamped rotor under constant acceleration and symmetrically supported on two identical bearings would be

$$\left(\frac{r}{e}\right)_{\text{maximum}} = 1.5 \frac{\omega_n}{\sqrt{a}} \tag{46}$$

where a is the ratio of an applied torque to the polar inertia of the rotor, or the balanced angular acceleration of the rotor.

Equation (46) suggests that for a rotor-bearing system with substantial angular acceleration capacity, the effects of acceleration on minimizing the rotor deflection, and consequently the bearing reactions, can be significant.

Although a basic rule in minimizing the steady-state rotor deflection and bearing reactions at or near a critical speed is to provide low bearing mount stiffness and an adequate amount of damping, a general formulation to determine the optimum requirements for a practically unlimited number of rotor-bearing configurations would be quite complex. Fortunately, the optimum bearing mount characteristics for a rotor-bearing system can be determined with accuracy by the application of generally available axisymmetric critical speed and rotordynamic response computer programs in a manner similar to that carried out by

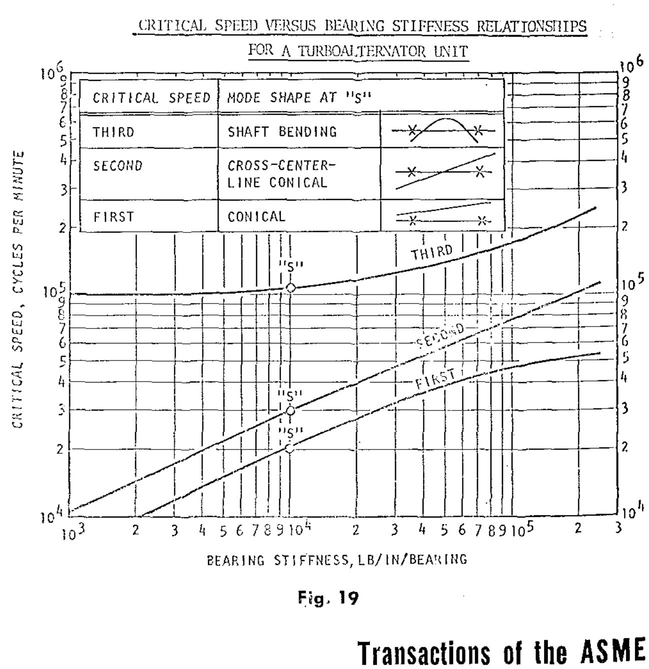

Fig. 19

[4] North American Rockwell Corporation, Rocketdyne Division, Canoga Park, Calif. Mem. ASME.

the author. The whirl driving component of a rotor-bearing system can be precisely represented by an appropriate negative damping parameter generally provided in the response computer program.

A critical speed versus bearing stiffness relationship from a past study of a high speed turboalternator is shown in the Fig. 19. This was a first step in minimizing the rotor deflection and bearing reactions in the critical speed regions.

While the first and second critical speed, as shown in the graph, are drastically lowered by using the low bearing or mount stiffness, the magnitude of the third critical speed, a shaft bending mode, is also materially affected by the bearing stiffness. In seeking a smooth operating speed range, the lowering of the third critical speed resulting from low bearing mounting stiffness should also be considered.

Additional Reference

18 Macchia, D., "Acceleration of an Unbalanced Rotor Through the Critical Speed," based on a Master's thesis at Cornell University (date of paper not available).

Author's Closure

The author greatly appreciates the interest and valuable comments of J. M. McGrew and F. A. Shen to this paper. In reply to Mr. McGrew, I would also like to point out the excellent work by Lund [19] on flexible rotor response, which also includes the effect of bearing support mass.

The equations to include the influence of the support mass have been developed and are presented in [20]. An extensive investigation on the effect of the support or bearing housing response on the rotor motion was conducted by the author and R. G. Kirk at the University of Virginia, and the results of this study are being prepared for publication. For example, Fig. 20 represents the rotor motion of a system in which the total bearing housing mass M_1 equals the rotor mass $M_2(M_1/M_2 = M = 1)$ and the support stiffness K_1 is equal to the effective bearing and rotor stiffness K_2. The dimensionless damping coefficient C represents the ratio of damping in the support to the effective damping in the bearing and rotor. For light values of support damping, two resonance frequencies are introduced on either side of the original critical speed. Note that if excessive support damping is used, then the support becomes ineffective in attenuating the rotor motion, resulting in high amplitudes at the critical speed. For each value of support housing mass and stiffness there is an optimum damping coefficient for maximum rotor attenuation and minimum bearing forces. Fig. 21 represents the dimensionless rotor amplitude versus the support to bearing damping ratio for various stiffness ratios for the case where the total support mass is 0.1 of the rotor mass. The value of $A = 10$ represents the rotor amplification factor at the critical speed on rigid supports. Note that when the support stiffness is twice the bearing stiffness ($K = 2$) the optimum damping in the support must be 30 times greater than the bearing damping to reduce the amplification factor to 3.5. If a very soft support system is used ($K = 0.01$) then the optimum support system damping value may vary over a wide range from 0.5 to 5 times the bearing damping value to achieve an amplification factor of less than 1.5, as compared to 10 for the rigid support case.

The orbits in Figs. 13 and 14 were obtained, not with a linear spring-damper system, but by integrating the forces as predicted by the nonlinear Reynolds equation with the dynamical system equations of motion. The form of the Reynolds equation used for the squeeze film bearing is as follows:

$$\frac{1}{R^2}\frac{\partial}{\partial\theta}\left(\frac{h^3}{\mu}\frac{\partial p}{\partial\theta}\right) + \frac{\partial}{\partial z}\left(\frac{h^3}{\mu}\frac{\partial p}{\partial z}\right) = 12\frac{dh}{dt} \qquad (47)$$

Various methods for the numerical solution of this equation are given by Castelli and Pirvics [21]. A typical hydrodynamical pressure distribution in the squeeze film bearing, including cavitation, is shown in Fig. 22 and is discussed in detail in [22]. The fluid film extent is dependent upon the instantaneous conditions of displacement and velocity, and only for the case of circular synchronous motion about the origin or squeeze film bearing center will the film be 180 deg. Feeding conditions will also have an effect on the performance since it will effect the bearing pressure distribution and cavitation region.

The particular dimensions of the squeeze bearing used in Figs. 13 and 14 were chosen to simulate the desired optimum damping coefficient of 6.7 for small unbalance values [23]. This damping coefficient may be adequately approximated by the short bearing theory as presented by McGrew. The approximate damping co-

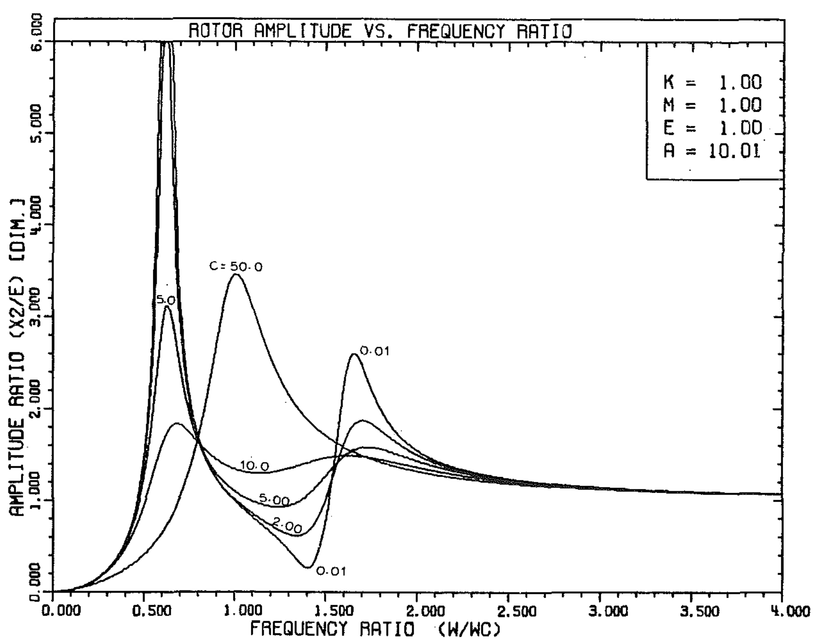

Fig. 20 Rotor amplitude versus dim rotor speed for various values of support damping (support to rotor mass ratio = 1)

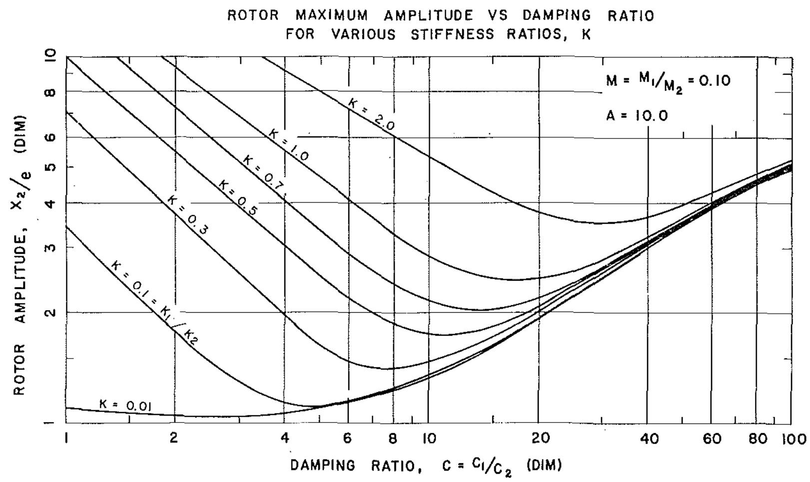

Fig. 21 Rotor maximum amplitude versus damping ratio for various stiffness ratios ($M = 0.10$)

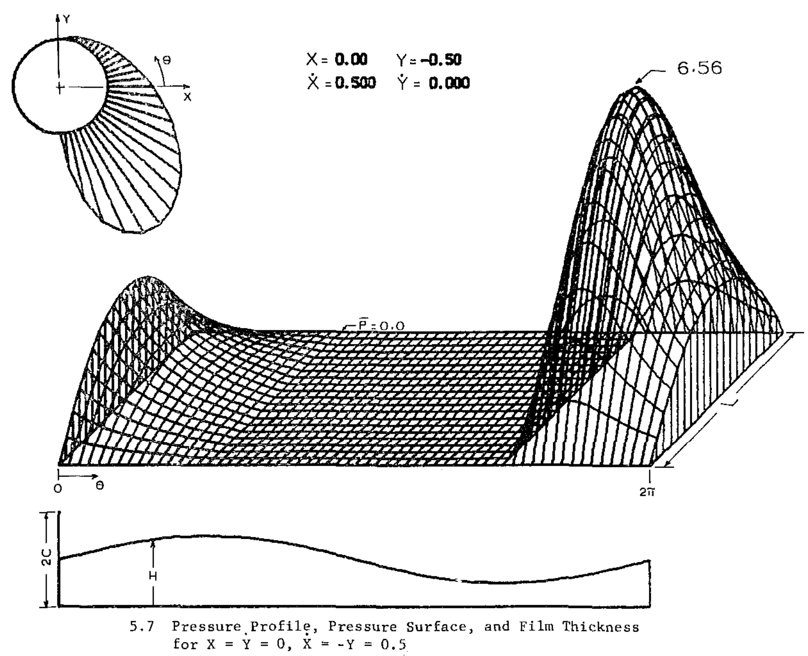

Fig. 22 Typical hydrodynamic squeeze film pressure profile including *cavitation*

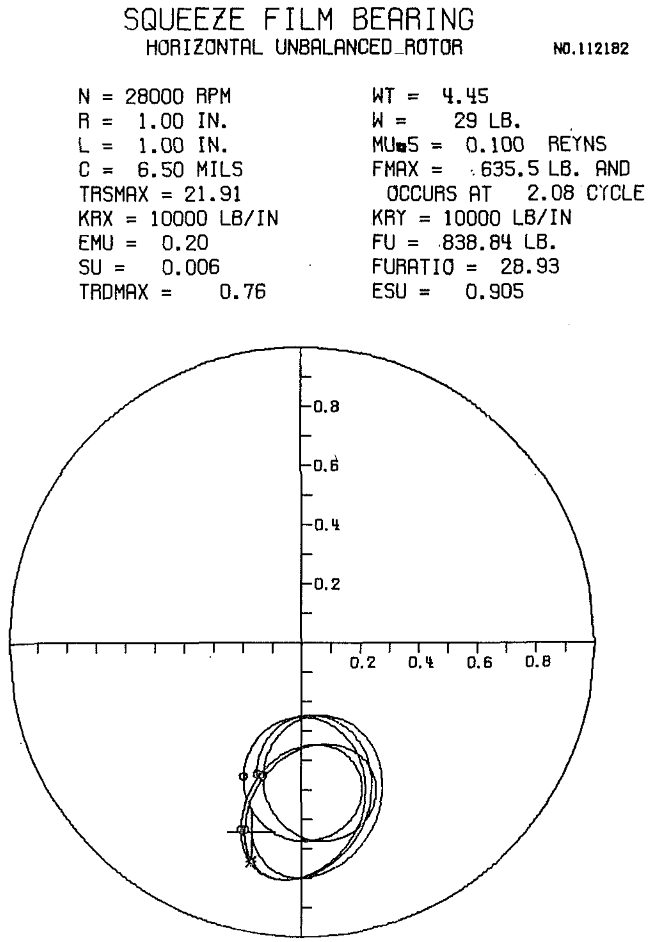

Fig. 23 Rotor motion in a squeeze film bearing after 20 cycles with vertical loading

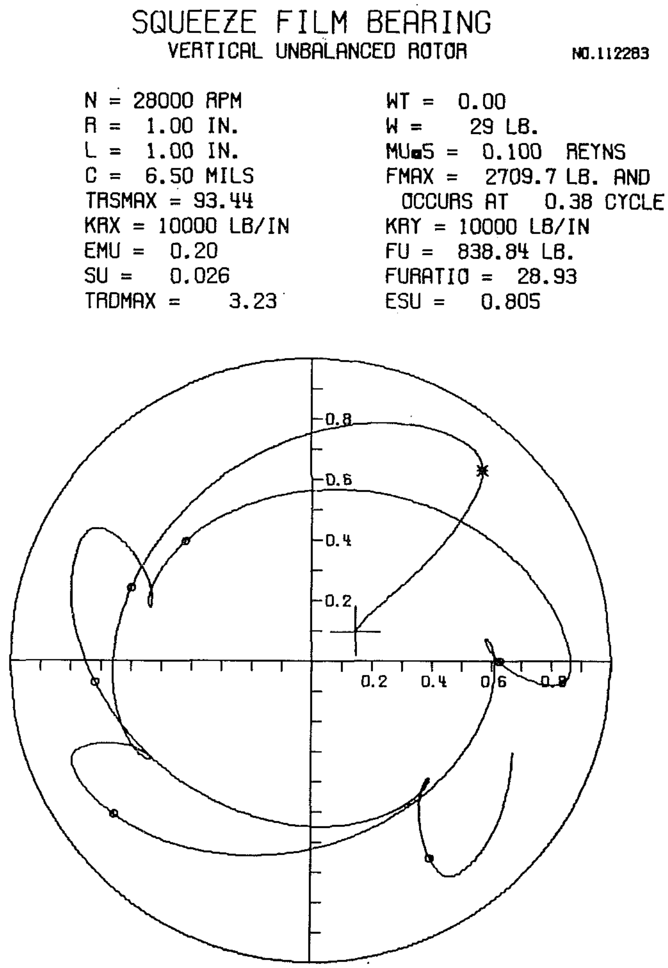

Fig. 24 Initial transient-motion of a rotor in a squeeze film with suddenly applied shock load

efficient is calculated by equation (37) as follows: Assuming $\epsilon_0 = 0.2$

$$C_0 = \frac{\mu L^3 R}{2C^3} \frac{\pi}{(1 - \epsilon_0^2)^{3/2}} = \frac{1 \times 10^{-6} \times 1^3 \times 1 \times 3.14}{2 \times (0.0005)^3 \times (1 - 0.2^2)^{3/2}} = 6.1$$

If the rotor is operated with external unidirectional loads, the motion is not purely circular synchronous about the origin and the squeeze film contribution due to the ϵ term can not be ignored. For example, Fig. 23 is identical to Fig. 14 but with the addition of a 100-lb vertical load. Note that the motion is no longer circular about the origin but has developed a subharmonic $^1/_2$ frequency component (not to be confused with $^1/_2$ frequency whirl encountered in plain bearings) due to the nonlinear bearing forces. The force transmitted has increased by a factor of 9 from only 70 lb to over 635 lb due to this slight unidirectional loading.

If the squeeze film damper is to be confidently incorporated in aviation gas turbines, then the author believes that further nonlinear transient analysis of this system is required. Fig. 24 represents the shaft motion caused by a suddenly applied shock load on the system. Note that the motion does not damp out nicely as was the case with the suddenly applied unbalance in Fig. 13; a large sustained transient orbit has been developed causing a transmitted force of over 2700 lb. The occurrence of such a motion in an actual operating system could be disasterous.

Additional References

19 Lund, J. W., "Rotor-Bearing Dynamics Design Technology—Part V," Technical Report AFAPL—TR-65-45, May 1965, Aero Propulsion Lab., Wright-Patterson Air Force Base, Dayton, Ohio.

20 Gunter, E. J., and P. De Choudhury, "Rigid Rotor Dynamics," NASA Report CR-1391, Aug. 1969.

21 Castelli, V., and Pirvics, J., "Review of Numerical Methods in Gas Bearing Film Analysis," JOURNAL OF LUBRICATION TECHNOLOGY, TRANS. ASME, Series F, Vol. 90, No. 4, Oct. 1968, pp. 777–792.

22 Kirk, R. G., "Transient Journal Bearing Analysis," Masters Thesis, Department of Mechanical Engineering, University of Virginia, Charlottesville, Va., June 1969, 198 pp.

23 Horner, G., "The Dynamic Characteristics of a Floating Squeeze Film Bearing," Masters Thesis, Department of Mechanical Engineering, University of Virginia, Charlottesville, Va., Jan. 1968.